

# Spinal cord MRS in and beyond the cervical spine

A. Henning<sup>1</sup>, M. Schär<sup>1,2</sup>, S. Kollias<sup>3</sup>, D. Meier<sup>1</sup>, P. Boesiger<sup>1</sup>, U. Dydak<sup>1</sup>

<sup>1</sup>Institute for Biomedical Engineering, University and ETH Zurich, Zurich, Kanton Zurich, Switzerland, <sup>2</sup>John Hopkins University, Baltimore, MD, United States, <sup>3</sup>Neuroradiology, Universital Hospital Zurich, Zurich, Kanton Zurich, Switzerland

## Introduction

MRS non-invasively gives insight into the metabolism of neuronal tissue and can provide valuable information regarding the differential diagnosis of space-occupying lesions. While MRS is therefore increasingly applied in the human brain, spinal cord MRS has been rarely used. It has been mainly restricted to the brain-stem and the upper part of the cervical spine [1, 2]. Furthermore, the quality of spectra has not been sufficiently reproducible and consistent to do patient measurements for clinical diagnostics. In this work, first MRS patient data from the thoracic spinal cord are shown. Moreover, the spectral quality as well as the consistency of MRS in the cervical spine was improved combining outer-volume suppression bands with a very sharp excitation profile, based on quadratic-phase (QPP) and higher-order-phase (HOPP) saturation pulses, and localized higher-order shimming, based on high-resolution cardiac-triggered static magnetic field  $B_0$ -mapping. The examples of a glioblastoma metastasis in the thoracic spinal cord as well as a multiple sclerosis plaque in the cervical spinal cord underline the diagnostic value of spinal cord MRS.

## Materials and Methods

All MRI and MRS experiments were performed on a Philips 3T scanner (Philips Medical Systems, Best, The Netherlands). In MRS the effective voxel size was  $6 \times 7 \times 27$  mm, TE was either 42 ms or 144 ms, and 512 averages were acquired over a bandwidth of 2000 Hz. Slightly over-prescribed PRESS (-1.5 mm) was combined with outer volume suppression based on HOPP or QPP saturation pulses [2], which were applied prior to the PRESS excitation. Pulse duration and flip angle of each suppression band were separately adjustable. Using Bloch simulation flip angles and number of suppression cycles have been optimized to simultaneously suppress fat and CSF. To saturate signal coming from the pulsatile flow of the CSF additional suppression slabs superior and inferior to the voxel have been applied and ECG triggering (300ms delay) was performed during the MRS acquisition. Localized second order shimming based on high-resolution ( $128 \times 128$ ) ECG-triggered  $B_0$ -mapping was applied prior to the MRS measurement.

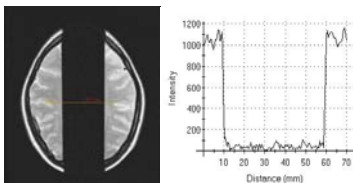


**Figure 1** Excitation profile of a higher order phase saturation pulse

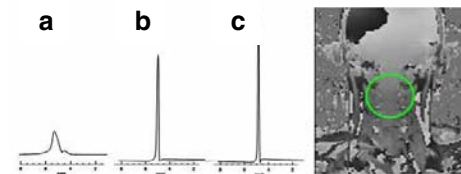


**Figure 2** Improved shim a) 1<sup>st</sup> order shim; 2<sup>nd</sup> order shim b) w/o; c) with ECG triggering; d)  $B_0$ -map

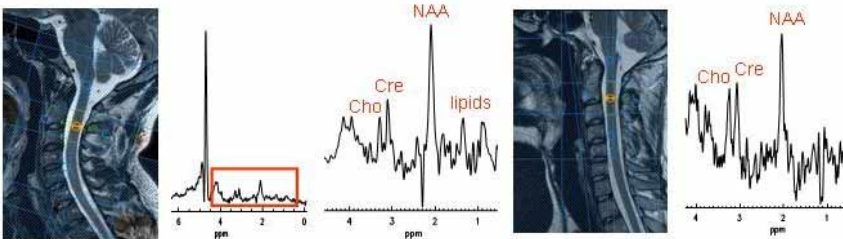


**Figure 3** Consistently high spectral quality acquired in the healthy cervical spine (C2/3) with TE = 42 ms. Blue bars around prescribed voxel show the position of saturation slabs.

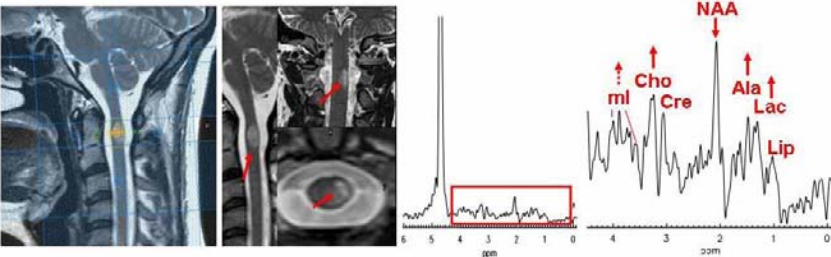


**Figure 4** Active demyelination in the cervical spine in a patient with multiple sclerosis (red arrows): TE = 42 ms

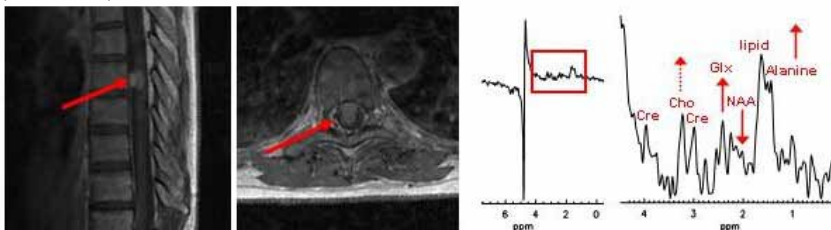


**Figure 5** High grade glioma in the thoracic spinal cord (red arrows): TE = 144ms

## Results and Discussion

Spinal cord single voxel spectra were acquired in the cervical, the thoracic as well as the lumbar spinal cord. The extremely sharp excitation profile of the QPP and HOPP saturation pulses (Figure 1) allowed the use of slightly over-prescribed PRESS, and therefore the avoidance of signal loss and CSF flow artifacts due to chemical shift displacement. A localized higher order shim routine based on ECG-triggered  $B_0$ -mapping improved the shim significantly (Figure 2) and ensured a reproducible water line width of 7 Hz in the cervical spinal cord. ECG-triggering was essential during the acquisition of the  $B_0$ -map as well as of the MR spectrum to achieve spectra with narrow, distinguished lines and hence sufficient SNR in the cervical spine. Figure 3 shows cervical spinal cord MR spectra at the level of C2 / C3 in two different healthy volunteers. Equally high spectral quality was consistently achieved over all five measured healthy volunteers as well as in a patient with a lesion at the level C1 / C2 (Figure 4). The patient spectrum shows increased Choline, Alanine, Lactate and myo-Inositol along with decreased NAA and therefore indicates an active demyelination due to multiple sclerosis.

Figure 5 shows a patient spectrum of a lesion in the lower thoracic spine. It was recorded with QPP-based outer volume suppression but without ECG-triggering. In spite of this, a water line width of 10 Hz and hence narrow, distinguished metabolite peaks with sufficient SNR were achieved. As shown on the T1 weighted images the lesion occupies almost the entire spinal cord canal and therefore significantly reduces CSF flow in this area, which enabled the high spectral quality. The spectrum shows increased Choline, Glutamate, lipids and Alanine along with decreased NAA and indicates a high grade glioma.

In spite of applying cardiac triggering, water line widths below 20 Hz could not be achieved in the healthy thoracic and lumbar spine. According to Friese [4] the pulsatile CSF flow induced by cardiac motion is strongest in the brain stem and in the cervical spine and almost negligible in the thoracic and lumbar spine, where CSF flow is rather caused by respiratory motion. Therefore one may hypothesize that respiratory gating is necessary to achieve a good shim, and hence good spectral quality, in the healthy thoracic and lumbar spine, while it was shown that space-occupying lesions are accessible to MRS without respiratory gating.

## References

- [1] Cooke, et al., MRM 2004; 51: 1122-1128  
 [2] Dydak, et al., Proc. ISMRM 2005; 13: 813  
 [3] Schulte, et al., JMR 2004 ; 166: 111-122  
 [4] Friese, et al., Klin Neuroradiol 2002; 12:67-75